

# Molecular Recognition in Cyclodextrin Complexes of Amino Acid Derivatives. 1. Crystallographic Studies of $\beta$ -Cyclodextrin Complexes with *N*-Acetyl-L-phenylalanine Methyl Ester and *N*-Acetyl-L-phenylalanine Amide Pseudopeptides

Joanna L. Clark and John J. Stezowski \*

Contribution from the Department of Chemistry, University of Nebraska—Lincoln, Lincoln, Nebraska 68588-0304

Received October 18, 2000

**Abstract:** Cyclodextrins (CDs) are widely utilized in studies of chiral and molecular recognition. By changing the functionality of the guest molecule, the effect of such changes on recognition by the host CD molecule can be examined. We report crystal structure determinations for two nearly isomorphous complexes of phenylalanine derivatives:  $\beta$ -CD/*N*-acetyl-L-phenylalanine methyl ester and  $\beta$ -CD/*N*-acetyl-L-phenylalanine amide. The complexes crystallize as hydrated head-to-head host dimers with two included guest molecules in space group *P*1. The crystal packing is such that it presents a nonconstraining hydrophobic pocket adjacent to a hydrophilic region, where potential hydrogen-bonding interactions with hydroxyl groups of neighboring cyclodextrin molecules and waters of hydration can occur. The two host molecules display very similar conformations; only a few of the primary hydroxyl groups are conformationally disordered. There are a number of changes in the location of water of hydration molecules, some of which are the result of different hydrogen-bonding interactions. For the different guest molecules, similar modes of penetration are observed in the CD torus; however, there is a 0.985-Å shift in the position of the guest molecules in the host torus, which takes place without changing the hydrophobic interactions displayed by the phenyl side chains. This observation and the thermal motion of the guest molecules in the ester complex are taken as evidence that complex binding forces are weak. The pseudopeptides experience a significant degree of flexibility in the crystalline environment provided by CD dimers. Conformational differences of the pseudopeptide backbones and the presence of disordered water molecules in the host–guest interface provide examples of different hydrogen-bonding schemes of similar potential energy. The crystal system presents an opportunity to establish a database of molecular interactions for small peptides and peptide analogues with waters of hydration and functional groups in nonconstraining binding environments.

## Introduction

Cyclodextrins (CDs) are naturally occurring oligomers of  $\alpha$ -1,4-linked D-glucose units. Their chemical structure presents a hydrophobic cavity that can encapsulate various guest molecules to produce supramolecular inclusion complexes. Consequently, they are ideal prototypes for examining intermolecular interactions associated with molecular and chiral recognition.<sup>1–4</sup> Native  $\beta$ -CD (seven D-glucose units) and synthetic derivatives of  $\beta$ -CD are widely utilized in chromatographic applications<sup>5,6</sup> and have potential application as drug carriers,<sup>7</sup> providing an incentive to better understand the unique nonbonding interactions associated with their recognition of guest molecules. Crystallographic studies provide direct access to this type of structural information.

\* To whom correspondence should be addressed. E-mail: jstezowski1@unl.edu.

- (1) Schneider, W. *Agnew. Chem., Int. Ed.* **1991**, *30*, 1417–1436.
- (2) Harata, K. *Chem. Rev.* **1998**, *98*, 1803–1827.
- (3) Szejtli, J. In *Comprehensive Supramolecular Chemistry*; Pergamon: Oxford, U.K., 1996; pp 189–203.
- (4) Easton, C. J.; Lincoln, S. F. *Chem. Soc. Rev.* **1996**, 163–170.
- (5) Armstrong, D. W.; Ward, T. J.; Armstrong, R. D.; Beesley, T. E. *Science* **1996**, *232*, 1132–1135.
- (6) Armstrong, D. W. *J. Liq. Chromatogr.* **1984**, *7* (S-2), 355–376.
- (7) Uekama, K.; Hirayama, F.; Irie, T. *Chem. Rev.* **1998**, *98*, 2045–2076.

Several recent works report solution studies of CD complexes of amino acids, their derivatives, and small peptides, using a variety of methods such as mass spectrometry, UV/visible spectrometry, and microcalorimetry.<sup>8–14</sup> These studies, directed toward an understanding of thermodynamic aspects of binding and chiral discrimination in CDs, have provided valuable information on the effects of changes in functionality and chirality on molecular recognition. In one particular work,  $\beta$ -CD was used to model the receptor–peptide (protein–ligand) interaction of two different neural peptides.<sup>15</sup> Most of the solution-state work has been conducted under the assumption that complexes associate with 1:1 stoichiometry.

- (8) Liu, Y.; Zhang, Y.; Sun, S.; Li, Y.; Chen, R. *J. Chem. Soc., Perskin Trans. 2* **1997**, 1609–1613.
- (9) Liu, Y.; Li, B.; Han, B.; Li, Y.; Chen, R. *J. Chem. Soc., Perskin Trans. 2* **1997**, 1275–1278.
- (10) Rekharsky, M. V.; Inoue, Y. *J. Am. Chem. Soc.* **2000**, *122*, 4418–4435.
- (11) Rekharsky, M. V.; Schwarz, F. P.; Tewari, Y. B.; Goldberg, R. N. *J. Phys. Chem.* **1994**, *98*, 10282–10288.
- (12) Horský, J.; Pitha, J. *J. Inclusion Phenom. Mol. Recognit. Chem.* **1994**, *18*, 291–300.
- (13) Lipkowitz, K. B.; Raghothama, S.; Yang, J. *J. Am. Chem. Soc.* **1992**, *114*, 1554–1562.
- (14) Maletic, M.; Wennemers, H.; McDonald, D. Q.; Breslow, R.; Still, W. C. *Angew. Chem., Int. Ed. Engl.* **1996**, *35*, 1490–1492.
- (15) Bekos, E. J.; Gardella, J. A.; Bright, F. V. *J. Inclusion Phenom. Mol. Recognit.* **1996**, *26*, 185–195.

Despite the high level of interest in characterizing CD complexes of amino acids and their derivatives indicated by the solution studies, there are no reported solid-state studies of these systems. Systematic crystallographic studies can provide valuable insight into the intermolecular interactions involved in molecular recognition, especially when crystal-packing effects do not appear to unduly influence those interactions. CD complexes associate through noncovalent interactions such as hydrogen bonding, van der Waals forces, and electrostatic interactions. Historically, there has been a small collection of molecular recognition studies of CD complexes in the solid state. Geometric complementarity, or spatial fit, between host and guest has been suggested as one of the first requirements for molecular recognition by CDs,<sup>2</sup> although the relevance of other interactions has also been illustrated. A few previous crystallographic studies of CD complexes have shown that hydrogen-bonding interactions between the guest and CD primary hydroxyls or waters can also be important to molecular and chiral recognition.<sup>16–19</sup>

By comparing pseudopeptide complexes with small perturbations in guest backbone functional groups, we hope to gain an improved understanding of the importance of hydrogen-bonding and hydrophobic interactions to molecular recognition. We report structures of two different, crystallographically isomorphous  $\beta$ -CD complexes with *N*-acetyl-L-phenylalanine methyl ester (*N*-Ac-L-FOMe) and *N*-acetyl-L-phenylalanine amide (*N*-Ac-L-FNH<sub>2</sub>). The crystal structures provide a unique opportunity to observe a variety of molecular interactions in a relatively constant crystal lattice environment. The CD host molecules are associated through hydrogen bonding between secondary hydroxyl groups as dimers, packing in the previously observed Im packing arrangement.<sup>20–22</sup> The fact that this arrangement is common to these complexes of  $\beta$ -CD is important for two reasons: (a) it implies that crystal packing does not severely limit conformational and translational freedom of guest molecules, and (b) it provides an environment for the guest molecules that resembles a macromolecular binding pocket by providing a hydrophobic pocket rimmed with a scaffolding of hydrophilic binding sites that can interact directly with guest molecules or via bridging water molecules. As a consequence, guest molecules experience considerable variation in their specific interactions with the host molecules and waters of hydration, often resulting in the observation of crystallographic disorder.

This “loose” binding environment in the supramolecular  $\beta$ -CD complex crystals differs from that observed in a typical small molecule crystal, where crystal packing results from molecular interactions that determine lattice packing. It more closely resembles the binding environment typically observed in macromolecular crystals, where substrate molecules experience more complexity in their intermolecular interactions. However, structural aspects in macromolecular crystals are typically observed at much lower resolution, discouraging deconvolution

of disorder. We believe crystallographic studies of appropriate  $\beta$ -CD supramolecular inclusion complexes can provide improved insight on subtle differences in intermolecular interactions of similar energy; such interactions are commonly associated with molecular recognition. The system provides an unusual opportunity to study variations in intermolecular interactions at high resolution. The choice of the pseudopeptides as guest molecules enhances the value of the observations by increasing the biochemical significance to the system. We examine the intermolecular interactions in terms of (a) a somewhat nonspecific, nonconstraining hydrophobic pocket (the CD dimer) and (b) guest molecule hydrogen-bonding interactions with functional groups on neighboring host molecules, typically mediated by waters of hydration. With these considerations in mind, this system is expected to provide relevant information for those interested in molecular modeling of intermolecular interactions associated with molecular recognition, for example, in macromolecule–small molecule systems.

## Experimental Section

The complexes were prepared by combining a 1:1 molar ratio of  $\beta$ -CD (Cerestar) with *N*-Ac-L-FOMe or *N*-Ac-L-FNH<sub>2</sub> (Advanced ChemTech) in aqueous solution and heating gently. Single platelike parallelepiped crystals of the complexes were grown by slow evaporation at room temperature.

**Crystallographic Data for the *N*-Ac-L-FOMe/ $\beta$ -CD Complex at 297 K.** A  $0.7 \times 0.7 \times 0.7$  mm<sup>3</sup> crystal of *N*-Ac-L-FOMe/ $\beta$ -CD complex (2C<sub>42</sub>H<sub>70</sub>O<sub>35</sub>·2C<sub>12</sub>H<sub>15</sub>O<sub>3</sub>N<sub>1</sub>·23.35H<sub>2</sub>O) was sealed in a thin-walled glass capillary with mother liquor. Diffraction data were measured with a Syntex P1 autodiffractometer ( $\lambda = \text{Mo K}\alpha$ ); unit cell constants are  $a = 18.129(2)$ ,  $b = 15.411(2)$ , and  $c = 15.585(2)$  Å,  $\alpha = 103.97(1)^\circ$ ,  $\beta = 112.89(1)^\circ$ ,  $\gamma = 98.79(1)^\circ$ , and  $V = 3741.7$  Å<sup>3</sup>. Intensities for 13 217 unique reflections were collected to a resolution of 0.84 Å using an  $\omega$ -scan mode. The data were corrected for Lorentz and polarization effects, but not absorption ( $\mu = 0.125$  mm<sup>-1</sup>). A solution to the phase problem was obtained using the coordinates of the  $\beta$ -CD molecules from the isomorphous 1-propanol complex.<sup>23</sup> Least-squares refinement on  $F^2$  was carried out for 1648 parameters and 67 restraints using SHELXL97<sup>24</sup> and converged to a final  $R_1 = 0.079$ ,  $wR_2 = 0.235$ , and  $\text{GO}F = 1.040$  for 10 224 reflections with  $F_o > 4\sigma F_o$ . For the cyclodextrin, all non-hydrogen atoms were refined anisotropically. If possible, hydrogens were located in difference Fourier maps, otherwise hydrogens on carbons were generated geometrically and fixed in a riding model.

Waters of hydration were located in difference electron density maps ( $F_o - F_c$ ). Six well-ordered waters were refined with anisotropic atomic displacement parameters (ADPs), and 17.35 disordered waters distributed over 44 sites were refined isotropically. Inspection of electron density difference maps revealed significant disorder in the guest region, indicating possible thermal motion of the guest. Two guest molecules were incorporated per monomer in order to account for the disorder, and refined as rigid bodies, with restrained isotropic displacement parameters. A final ( $F_o - F_c$ ) map showed  $\rho_{\text{max}} = 0.624$ ,  $\rho_{\text{min}} = -0.628$ .

**Crystallographic Data for the *N*-Acetyl-L-FNH<sub>2</sub>/ $\beta$ -CD Complex at 297 K.** Data were measured using a Bruker AXS molybdenum target rotating anode X-ray source and an 18-cm Mar image plate detector. A  $0.9 \times 0.9 \times 0.7$  mm<sup>3</sup> parallelepiped crystal of the *N*-acetyl-L-FNH<sub>2</sub>/ $\beta$ -CD complex (2C<sub>42</sub>H<sub>70</sub>O<sub>35</sub>·2C<sub>12</sub>H<sub>14</sub>O<sub>2</sub>N<sub>1</sub>·23H<sub>2</sub>O), with lattice parameters  $a = 18.12(6)$ ,  $b = 15.40(6)$ , and  $c = 15.53(6)$  Å,  $\alpha = 103.32(6)^\circ$ ,  $\beta = 112.86(6)^\circ$ ,  $\gamma = 99.22(6)^\circ$ ,<sup>25</sup> and  $V^3 = 3732.3$  Å<sup>3</sup> was sealed in a thin-walled glass capillary with mother liquor for data collection.

(23) Stezowski, J. J.; Jogun, K. H.; Eckle, E.; Bartels, K. *Nature* **1978**, *274*, 617–618.

(24) Sheldrick, G. M. *SHELXL97. Program for the Refinement of Crystal Structures*, University of Göttingen, Germany, 1997.

(25) Esds from imaging plate data are typically greater than those from 4-circle diffractometer measurements: Perakakis, A.; Schneider, T. R.; Antoniadou-Vyzas, E.; Dauter, Z.; Hamodrakas, S. J., *J. Appl. Cryst.* **1996**, *261*–264.

(16) Harata, K. *J. Chem. Soc., Perkins Trans. 2* **1990**, 799–804.

(17) Hamilton, J. A.; Chen, L. *J. Am. Chem. Soc.* **1988**, *110*, 5833–5841.

(18) Harata, K.; Hirayama, F.; Imai, T.; Uekama, K.; Otagiri, M. *Chem. Lett.* **1984**, 1549–1552.

(19) Harata, K.; Uekama, K.; Otagiri, M.; Hirayama, F. *Chem. Lett.* **1983**, 1807–1810.

(20) Saenger, W. In *Inclusion Compounds*; Atwood, J. L., Davies, J. E. D., MacNicol, D. D., Eds.; Academic Press: London, 1984; Vol. 2, pp 231–259.

(21) Mentzafos, D.; Mavridis, M.; LeBas, G.; Tsoucaris, G. *Acta Crystallogr., Sect. B* **1991**, *47*, 746–757.

(22) Brett, T. J.; Alexander, J. M.; Stezowski, J. J. *J. Chem. Soc., Perkin Trans. 2* **2000**, 1095–1103.

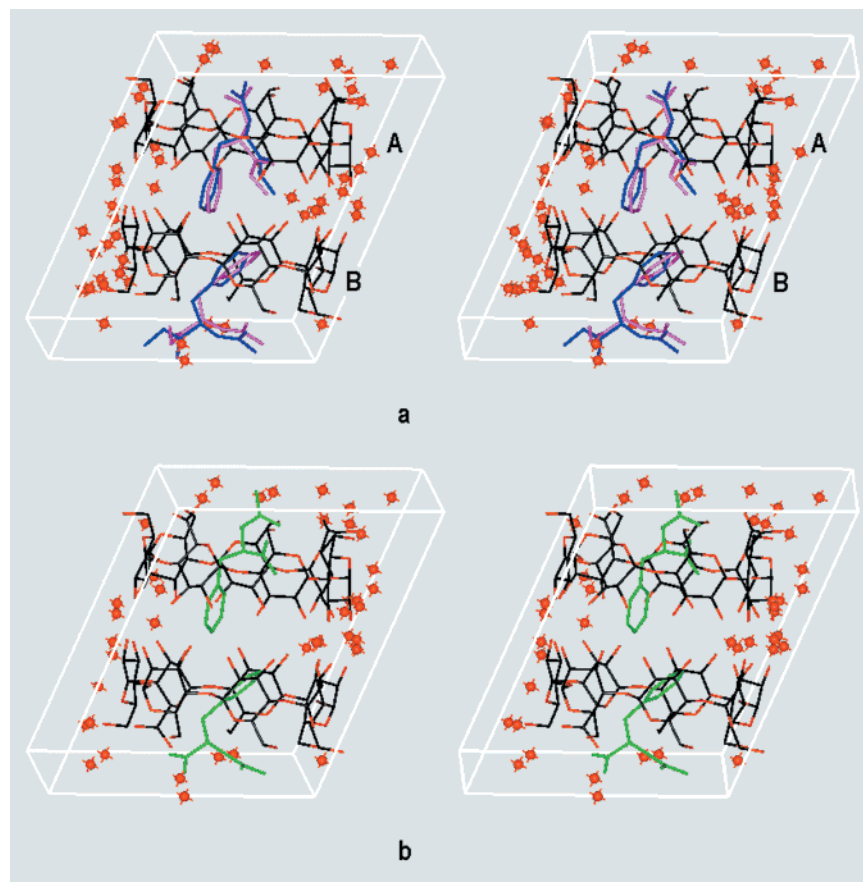


**Figure 1.** Stereoscopic projections illustrating the contents of one unit cell each for (a) the *N*-Ac-L-FOMe complex and (b) the *N*-Ac-L-FNH<sub>2</sub> complex. The disordered guest molecules in the *N*-Ac-L-FOMe complex are depicted in dark blue and magenta to facilitate recognition. The *N*-Ac-L-FNH<sub>2</sub> in (b) is green. The two projections have been prepared with the host cyclodextrin dimers in the same orientation to facilitate comparison. Water molecules of hydration are shown in red, and CD dimers are colored by atom type, with black carbon atoms and red oxygen atoms.

A total of 22 061 total reflections were collected by an oscillation method, yielding 12 425 unique reflections,  $R(\text{int}) = 0.026$ , to a resolution of 0.81 Å. The program MARXDS was used to process the data, which includes corrections for Lorentz and polarization effects.<sup>26</sup> An absorption correction was not applied ( $\mu = 0.124 \text{ mm}^{-1}$ ). A solution to the phase problem was obtained by isomorphous replacement of the  $\beta$ -CD coordinates from the *N*-Ac-L-FOMe complex. Least-squares refinement on  $F^2$  was carried out for 1722 parameters and 225 restraints using SHELXL97 and converged to a final  $R_1 = 0.084$ ,  $wR_2 = 0.22$ , and  $\text{GOF} = 1.06$  for 11 842 reflections with  $F_o > 4\sigma F_o$ . For the cyclodextrin, all non-hydrogen atoms were refined anisotropically. Hydrogens on carbons were generated geometrically and fixed in a riding model.

Waters of hydration were located in difference electron density maps ( $F_o - F_c$ ). Ten well-ordered waters were refined with anisotropic ADPs, and 13 disordered waters distributed over 31 sites were refined isotropically. Only one distinct guest site per monomer was observed in electron density difference maps. The guests were refined as rigid bodies. Unlike the above *N*-Ac-L-FOMe complex, where the amount of guest disorder precluded anisotropic refinement, these guest molecules were refined with restrained isotropic and anisotropic ADPs. A final ( $F_o - F_c$ ) map showed  $\rho_{\text{max}} = 0.74$ ,  $\rho_{\text{min}} = -0.71$ . Parst97 was used to examine and measure the distances of intermolecular interactions in these crystals.<sup>27</sup>

## Results and Discussion

The unit cell contents for both complexes are displayed in stereoscopic projection in Figure 1; an ORTEP plot illustrating refined thermal ellipsoids for all C, N, and O atoms at the 50%

probability level has been deposited. Atoms labels for the CD dimer are based on conventional glucose numbering. Figure 1a illustrates the monomers defined as **A** and **B**. For the **A** monomer, the CD residues are numbered 1–7, for the **B** monomer, 8–14. Primary hydroxyls are labeled as follows: O6-#, where the # is the residue number. Phenylalanine guest atoms are labeled with conventional amino acid labels. The acetyl nitrogen is labeled NAc, and acetyl carbonyl oxygen OAc. For the *N*-Ac-L-FOMe guests, the ester backbone carbonyl oxygen is labeled O. For the *N*-Ac-L-FNH<sub>2</sub> guests, the amide backbone carbonyl oxygen is labeled OAm and the amide nitrogen is labeled NAM. As mentioned above, the crystal structures are isomorphous; that is, both complexes crystallize in space group *P*1 with similar lattice parameters. The asymmetric unit (and unit cell) consists of head-to-head hydrogen-bonded  $\beta$ -CD dimer hosts; two included guest molecules, and several waters of hydration. The isomorphous nature of the two crystal structures is taken as evidence that the crystal-packing energies for the two structures do not differ dramatically. Consequently, similarities and differences observed in their three-dimensional structures primarily reflect molecular interactions relevant to molecular recognition.

Crystalline complexes of hydrogen-bonded  $\beta$ -cyclodextrin dimers complexed with organic guest molecules have been found previously to adopt one of four crystal packing motifs: a channel motif (Ch), a checker board motif (CB), an intermediate motif (Im), and, most recently, a tetrad motif (Tt). Packing diagrams are available in two different reports on  $\beta$ -cyclodextrin complexes; the reader is referred to these works for both

(26) Kabsch, W. *J. Appl. Crystallogr.* **1988**, 21, 916–924.

(27) Nardelli, M. *Comput. Chem.* **1983**, 7, 95–98.

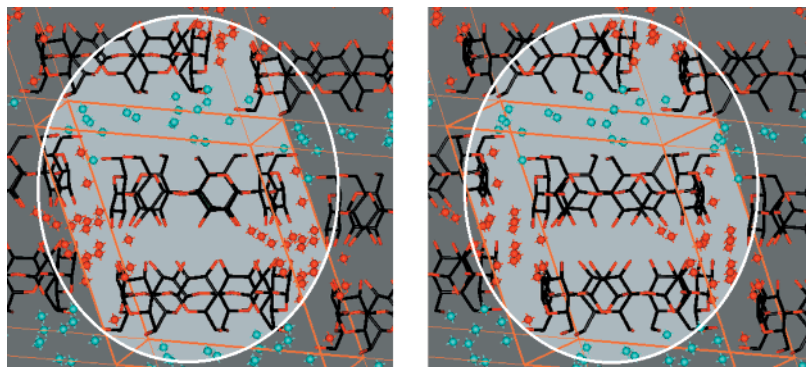


**Figure 2.** Stereoscopic projection illustrating the Im packing as observed here. A “pocket” is provided by the Im packing motif of these  $\beta$ -CD complexes that has many properties of a macromolecular small-molecule binding site. The pocket is highlighted in the figure. The following features are noteworthy: (a) there is a nonconstraining, extended, torus formed by the hydrogen-bonded  $\beta$ -CD dimers (the central portion of the light gray area), (b) there are a number of water of hydration molecules in the hydrophilic interface between the sheets available to participate in intermolecular interactions between the binding pocket and the “guest” molecule (cyan), and (c) there are intrasheet pockets of space-filling water of hydration molecules that are not accessible to the guest molecules (red).

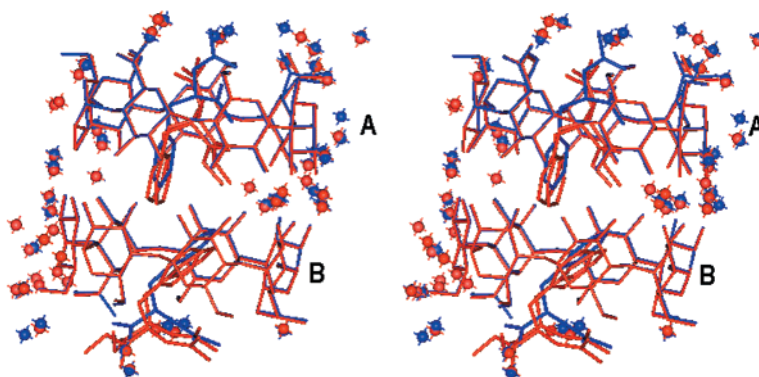


**Figure 3.** Color-coded stereoscopic superposition diagram of the contents of one unit cell for both complexes allowing a comparison of the guest positions, conformations, and orientations inside the CD dimer. The *N*-Ac-L-FOME/ $\beta$ -cyclodextrin complex is red, and the *N*-Ac-L-FNH<sub>2</sub>/ $\beta$ -cyclodextrin complex is blue.

diagrams and discussion of the different structural properties for these packing arrangements.<sup>20–22</sup> Illustrations have been deposited.

The complexes reported here adopt the Im packing motif. This arrangement presents a number of favorable properties for the study of molecular recognition at atomic resolution. Figure 2 illustrates features of the crystal packing (in stereoscopic projections based on the crystal structure of the methyl ester complex) that are relevant to the use of this system as a matrix for the study of molecular recognition. The crystal structure of the Im packing motif may be viewed as consisting of stacked sheets of hydrated hydrogen-bonded dimers. The packing in the sheets approximates close packed cylinders (the  $\beta$ -CD hydrogen-bonded dimers) in contact along the crystallographic *b*- and *c*-axes. The oxygen atoms drawn as red spheres in Figure 2 represent space-filling clusters of water molecules located in the sheets between the cylinders at the interface between four unit cells. The sheets are stacked along the crystallographic *a*-axis and are separated by a combination of a water layer and, in these current examples, by parts of the pseudopeptide backbones (illustrated and discussed below). The waters located in the hydrophilic region separating sheets of CD dimers are cyan in Figure 2. Variations are observed for the distribution of water of hydration molecules in this intersheet region.

The stereoscopic projection in Figure 2 illustrates three domains where a number of pertinent features of the crystal packing make it an interesting substrate-binding pocket model, one suitable for study at high resolution. The three domains consist of (a) a hydrogen-bonded  $\beta$ -CD dimer that presents guest

molecules with an extended hydrophobic toroidal void, (b) a scaffold of hydrogen-bonded donor–acceptor sites provided by neighboring  $\beta$ -CD molecules, and (c) a hydration sphere from which water molecules can mediate guest molecule receptor binding. The  $\beta$ -CD dimer may be appropriately regarded as a rigid container with little or no significant specific binding sites for included molecular moieties; it has been characterized as nonconstraining.<sup>28</sup> Within the sheets described above, these hydrophobic pockets may be regarded as isolated; guest molecules are not subject to significant attractive or repulsive forces from neighboring complexes. A number of space-filling water molecules (illustrated with red spheres at the positions of the oxygen atoms) between the close-packed  $\beta$ -CD dimers are separated by the host  $\beta$ -CD molecules from the guest molecules included in the torus. The hydrated interface between the sheets provides a hydrophilic region in the crystals consisting of primary hydroxyl groups of the  $\beta$ -CD molecules and water of hydration molecules (illustrated with cyan in Figure 2), which are available to mediate “receptor”–guest molecule interactions. As will be discussed below, crystallographic disorder, at times influenced by hydrogen-bonding interactions in this hydrated hydrophilic dimer interface region, can be observed for some of the pseudopeptide guest molecules in this binding environment.

The crystal structures of the pseudopeptide/ $\beta$ -CD inclusions are complex, with several different possibilities for guest molecule intermolecular interactions with disordered waters and

(28) Brett, T. J.; Lui, S.; Coppens, P.; Stezowski, J. *Chem. Commun.* **1999**, 551–552.

**Table 1.** Torsions Angles (deg) Characterizing the Pseudopeptide Guest Molecule Conformations<sup>a</sup>

torsion angle	N-Ac-L-FOMe		N-Ac-L-FNH <sub>2</sub>	N-Ac-L-FOMe		N-Ac-L-FNH <sub>2</sub>
	A1	A2	A	B1	B2	B
$\omega$	-177.82	176.59	-171.26	-179.38	175.54	-168.59
$\phi$	-167.86	-162.50	-55.02	-124.36	-135.79	-101.42
$\psi$	174.88	174.81	138.08	174.80	118.41	85.34
$\chi_1$	98.66	84.24	-172.84	-57.60	-45.10	-61.27
$\chi_2$	118.19	106.74	90.69	90.20	96.23	108.17

<sup>a</sup> **A** and **B** denote the monomer half in which the guest is included, as defined in Figures 1 and 4.

primary hydroxyls of the surrounding CD host dimers. In the discussion that follows, general similarities and differences in the conformations of the host system, the distribution of water of hydration molecules and the conformational similarities and differences of the guest molecules (Table 1) will be discussed first, followed by more detailed analysis of intermolecular interactions. Figure 3 is a color-coded, stereoscopic superposition diagram of the contents of one unit cell that helps to assess differences between the two complexes.

The host structures exhibit little conformational variability; differences are only observed in a small number of conformationally disordered primary hydroxyls; thus, description of the CD as a conformationally rigid molecule is appropriate. In both structures, primary hydroxyls O6(1) and O6(5) are disordered over two sites, one site a (+) gauche conformer (where the indicated primary hydroxyls point toward the interior of the CD) and the other a (-) gauche conformer (said hydroxyls point toward exterior). Three other primary hydroxyls, O6(9), O6(11), and O6(13), show signs of librational averaging, which was adequately modeled in the crystal structure determination with one hydroxyl site for each. The most prominent interactions between  $\beta$ -CD molecules are intermolecular hydrogen bonds between secondary hydroxyl groups, which give rise to the face-to-face dimer that is common to all four packing arrangements. Intermolecular contacts between these dimers give rise to the sheets in the Im packing motif. There are five interdimer hydrogen bonds between primary hydroxyl groups, Tables 2 and 3, four of which are intrasheet. Two of these are relevant to the binding pockets (discussed below). The fifth interdimer hydrogen bond is intersheet and thus contributes to the stability of the Im packing motif.

A number of the water of hydration molecules in the pockets between host dimers are disordered in a similar manner in the two crystal structures. It should be noted that the crystals crack and powder readily on standing in air in the absence of mother liquor. This is taken as an indication that the water molecules in the interstitial pockets assume primarily a space-filling role and are bound only loosely in the crystals. Beyond playing a role in determining the overall crystal structure, such water molecules are not considered to participate in host/substrate molecular recognition.

Figure 4 illustrates the electron density for the guest region of the extended torus for the two complexes. We interpret the electron density observed in the toroidal region of the N-Ac-L-FOMe complex as an indication of dynamic disorder, that is, thermal motion. We suggest that the two guest molecules fit to this density very likely represent "extreme" positions for the molecules undergoing thermal motion. In contrast, the electron densities for the atoms of the N-Ac-L-FNH<sub>2</sub> guest molecules are nearly spherical for all atoms of the molecule, which is an indication (a) that there is little thermal motion in the latter

**Table 2.** Parameters for Hydrogen-Bonding Interactions Observed in the N-Ac-L-F-OMe / $\beta$ -CD Complex

interaction <sup>a</sup>	distance (heavy atom to heavy atom) (Å)	populations (%) atom 1:atom 2
	O6(2)- -O6(6) ( $x,y,z - 1$ )	2.74(1)
O6(2)- -OAc( <b>B1</b> ) ( $x - 1,y,z - 1$ )	2.59(1)	100:50
O6(2)- -OAc( <b>B2</b> ) ( $x - 1,y,z - 1$ )	3.08(1)	100:50
w30d- -O6(3)	3.01(4)	50:100
w30c- -O6(3)	2.67(3)	50:100
w30d- -w29 ( $x,y,z - 1$ )	2.95(4)	50:100
w30c- -w29 ( $x,y,z - 1$ )	2.57 (3)	50:100
w26b- -w29	2.49(9)	35:100
O6(5a)- -NAc( <b>B1</b> )( $x - 1,y,z$ )	2.94(2)	40:50
O6(5a)- -O( <b>B1</b> )( $x - 1,y,z$ )	3.03(2)	40:50
O6(5b)- -w26b	2.82(8)	60:50
O6(5a)- -w26a	2.65(6)	40:50
O6(5b)- -w30c ( $x,y,z + 1$ )	3.21(4)	60:50
w26b- -w39b ( $x - 1,y,z$ )	2.74(6)	35:50
w26b- -w24	2.76(8)	35:100
w26a- -w24	2.93(6)	35:100
w39b- -NAc( <b>B2</b> )	2.82(5)	50:50
OAc( <b>A1</b> )- -w31b	2.87(3)	50:50
OAc( <b>A2</b> )- -w31a	2.50(2)	50:50
w31b- -O6(8) ( $x - 1,y,z - 1$ )	2.59(2)	50:100
w31a- -O6(8) ( $x - 1,y,z - 1$ )	2.84(3)	50:100
w31b- -w19 ( $x - 1,y,z - 1$ )	2.79(2)	50:100
w31a- -w19 ( $x - 1,y,z - 1$ )	2.88(2)	50:100
O6(12)- -w31b ( $x + 1,y,z$ )	2.84(3)	100:50
w19- -w18 ( $x,y,z + 1$ )	2.75(3)	100:100
O6(12)- -w18	2.73(2)	100:100
O6(12)- -O6(8) ( $x,y,z - 1$ )	3.20(1)	100:100
O6(8)- -w17 ( $x,y,z + 1$ )	2.78(1)	100:100
w17- -O6(11)	2.72(2)	100:100
w17- -w33 ( $x + 1,y,z$ )	2.79(1)	100:100
w33- -O6(9) ( $x - 1,y,z - 1$ )	2.78(1)	100:100
O6(1a)- -O6(9) ( $x - 1,y,z - 1$ )	2.88(2)	75:100
O6(1b)- -O6(9) ( $x - 1,y,z - 1$ )	2.77(3)	25:100
O6(4)- -O6(7) ( $x,y + 1,z$ )	2.95(1)	100:100
O6(10)- -O6(14) ( $x,y + 1,z$ )	2.76(2)	100:100
O6(1a)- -w19	2.74(4)	20:100
O6(14)- -w19	2.74(1)	100:100

<sup>a</sup> **A** and **B** denote the monomer half in which the guest is included, as defined in Figures 1 and 4.

complex and (b) that it is more strongly bound in the complex. The basis for this stronger bonding will be addressed in the discussion of intermolecular interactions.

Comparing the structures illustrated in Figures 3 and 4 reveals that the chemically similar guests display similar packing modes in the CD torus without significantly distorting the host system. They do, however, display significantly different degrees of penetration and thermal motion, as well as some conformational differences. On the basis of calculated midpoints for the phenyl rings, the pairs of guest molecules in the two crystal structures are shifted by 0.985 Å with respect to their positions in the toroidal void. Nonetheless, the phenyl rings in both complexes show similar packing arrangements and intermolecular interactions. The distance between the respective midpoints for the phenyl rings of the amide complex is 4.763 Å; the comparable distances for the two examples in the ester complex are 4.832 and 4.687 Å. It is noteworthy that the average value for the ester complex, 4.755 Å, is identical within experimental error to that in the more ordered amide complex. The geometries of the phenyl rings may be interpreted as indicative that there is meaningful attractive C-H $\cdots$  $\pi$ -cloud intermolecular interaction between the included guest molecules.

There are interesting similarities and differences in the conformations of the pseudopeptide backbones both within a single structure and when comparing them. As illustrated in

**Table 3.** Parameters for Hydrogen-Bonding Interactions Observed in the *N*-Ac-L-F-NH<sub>2</sub> / $\beta$ -CD Complex

interaction <sup>a</sup>	distance (heavy atom to heavy atom) (Å)	populations (%) atom 1:atom 2
O6(2)- -O6(6) ( <i>x,y,z</i> - 1)	2.74(1)	100:100
O6(2)- -OAc( <b>B1</b> ) ( <i>x</i> - 1, <i>y,z</i> - 1)	2.60(1)	100:100
w30- -O6(3)	2.70(2)	100:100
w30- -w29 ( <i>x,y,z</i> - 1)	2.65(3)	50:100
w26a- -w29	2.47(6)	40:100
O6(5a)- -w40b	2.80(9)	30:70
O6(5a)- -w26b	2.74(8)	30:35
O6(5b)- -w26a	2.84(6)	70:35
w26b- -w39b ( <i>x</i> - 1, <i>y,z</i> )	2.74(7)	35:50
w26a- -w24	2.81(6)	35:100
w26b- -w24	3.05(4)	35:100
w39b- -Nac( <b>B1</b> )	2.88(4)	50:100
W39a- -Nac( <b>B1</b> )	2.94(3)	50:100
W40a- -OAm( <b>B1</b> ) ( <i>x</i> - 1, <i>y,z</i> )	2.96(2)	35:100
W40b- -OAm( <b>B1</b> ) ( <i>x</i> - 1, <i>y,z</i> )	2.58(8)	65:100
W40a- -OAm( <b>A1</b> )	2.77(2)	35:100
W40b- -OAm( <b>A1</b> )	3.23(1)	65:100
OAc( <b>A1</b> )- -w31	2.90(1)	100:100
Oac( <b>A1</b> )- -Nam( <b>B1</b> ) ( <i>x</i> - 1, <i>y,z</i> )	3.09(1)	100:100
w31- -O6(8) ( <i>x</i> - 1, <i>y,z</i> - 1)	3.01(1)	100:100
w31- -w19 ( <i>x</i> - 1, <i>y,z</i> - 1)	2.90(1)	100:100
O6(12)- -w31 ( <i>x</i> + 1, <i>y,z</i> )	3.86(1)	100:100
w19- -w18 ( <i>x,y,z</i> + 1)	2.79(1)	100:100
O6(12)- -w18	2.72(1)	100:100
O6(12)- -O6(8) ( <i>x,y,z</i> - 1)	2.87(1)	100:100
O6(8)- -w17 ( <i>x,y,z</i> + 1)	2.70(1)	100:100
w17- -O6(11a)	2.76(1)	100:100
w17- -w33 ( <i>x</i> + 1, <i>y,z</i> )	2.79(1)	100:100
w33- -O6(9) ( <i>x</i> - 1, <i>y,z</i> - 1)	2.78(1)	100:100
O6(1a)- -O6(9) ( <i>x</i> - 1, <i>y,z</i> - 1)	2.93(1)	75:100
O6(1b)- -O6(9) ( <i>x</i> - 1, <i>y,z</i> - 1)	2.73(1)	25:100
O6(4)- -O6(7) ( <i>x,y</i> + 1, <i>z</i> )	3.00(1)	100:100
O6(10)- -O6(14) ( <i>x,y</i> + 1, <i>z</i> )	2.77(1)	100:100
O6(1a)- -w19	2.78(1)	40:100
O6(14)- -w19	2.75(1)	100:100

<sup>a</sup> **A** and **B** denote the monomer half in which the guest is included, as defined in Figures 1 and 4.

Figure 4, the molecular conformations of the *N*-Ac-L-FOME molecules differ dramatically when comparing the guest mol-

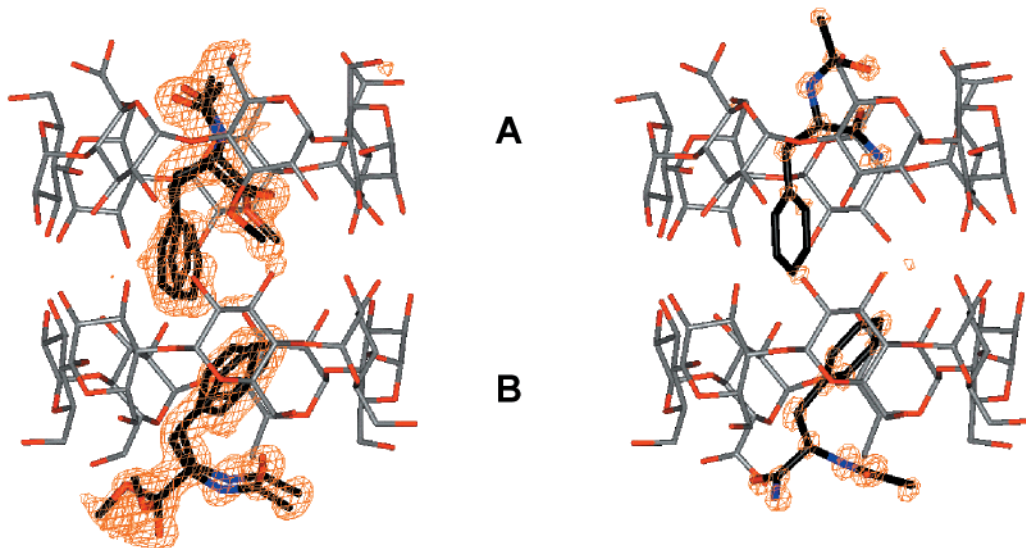


**Figure 4.** Difference electron density maps with the guest omitted superimposed over the modeled guests for the *N*-acetyl-L-phenylalanine methyl ester/ $\beta$ -cyclodextrin and *N*-acetyl-L-phenylalanine amide/ $\beta$ -cyclodextrin complexes. Hydrogen atoms on the CD and guests and waters are omitted for clarity. The electron density (gold) is calculated at  $0.6 \text{ e}^{-}/\text{\AA}^3$ . Differences in the nature of the electron density can be observed for the two complexes, with the *N*-Ac-L-FOME complex exhibiting more extensive disorder over the entire guest molecule region. This disorder was modeled with two guest sites per monomer. The guests modeled are possibly extremes of dynamic motion. In contrast, only one guest site per monomer was modeled for the *N*-Ac-L-FNH<sub>2</sub> complex, where the nature of the electron density was observed to be more sharp and spherical. CD dimers are colored by atom type, with gray carbon atoms and red oxygen atoms. Guest molecules are also colored by atom type, with black carbon atoms, blue nitrogen atoms, and red oxygen atoms.

ecules located in monomers **A** and **B**. Table 1 contains conventional torsion angles that describe the pseudopeptide guest molecule conformations. In **A**, the guest molecule backbone is in an extended conformation oriented such that the methyl ester is included deeply in the toroidal void of the host. In **B**, the guest molecule backbone is also generally extended, but is oriented to expose both the ester and the acetyl moieties to the interface between the sheets. For the *N*-Ac-L-FNH<sub>2</sub> guest molecules, the conformation of the **B** guest is similar to those of the ester; however, the **A** guest molecule backbone has a more folded conformation with the amide moiety oriented toward the sheet interface. As will be discussed below, this change in conformation allows the amide moiety to be involved in a few hydrogen bonds not found in the ester complex. Examination of Figure 4 reveals that, as a result of this conformational difference, there is also a significantly larger void in the torus of the host dimer in the amide complex than there is in the ester complex. It therefore appears that hydrophilic interactions play a more effective role in molecular recognition in the amide complex than in the ester complex.

The hydrophilic interactions, that is, hydrogen-bonding interactions, are found in the interface between sheets in the Im packing motif. They involve guest hydrogen bonds to host and water molecules, host-water interactions, and a couple of host-host hydrogen bonds. Disorder in the guest and water molecules also affects apparent hydrogen-bonding interactions. Figures 5 and 6 display the hydrogen-bonding interactions in the small-molecule binding environments for the ester and amide complexes, respectively. Tables 2 and 3 contain distances for interactions highlighted in Figures 5 and 6. In both complexes, there are two intermolecular hydroxyl hydrogen bonds directly between cyclodextrin molecules (O6(2)···O6(6) and O6(8)···O6(12)) that help define guest binding regions in the Im crystal packing motif.

The acetyl group, the common moiety in the backbone of the two pseudopeptides, has a carbonyl oxygen atom that can act as a hydrogen bond acceptor and an amide N-H moiety



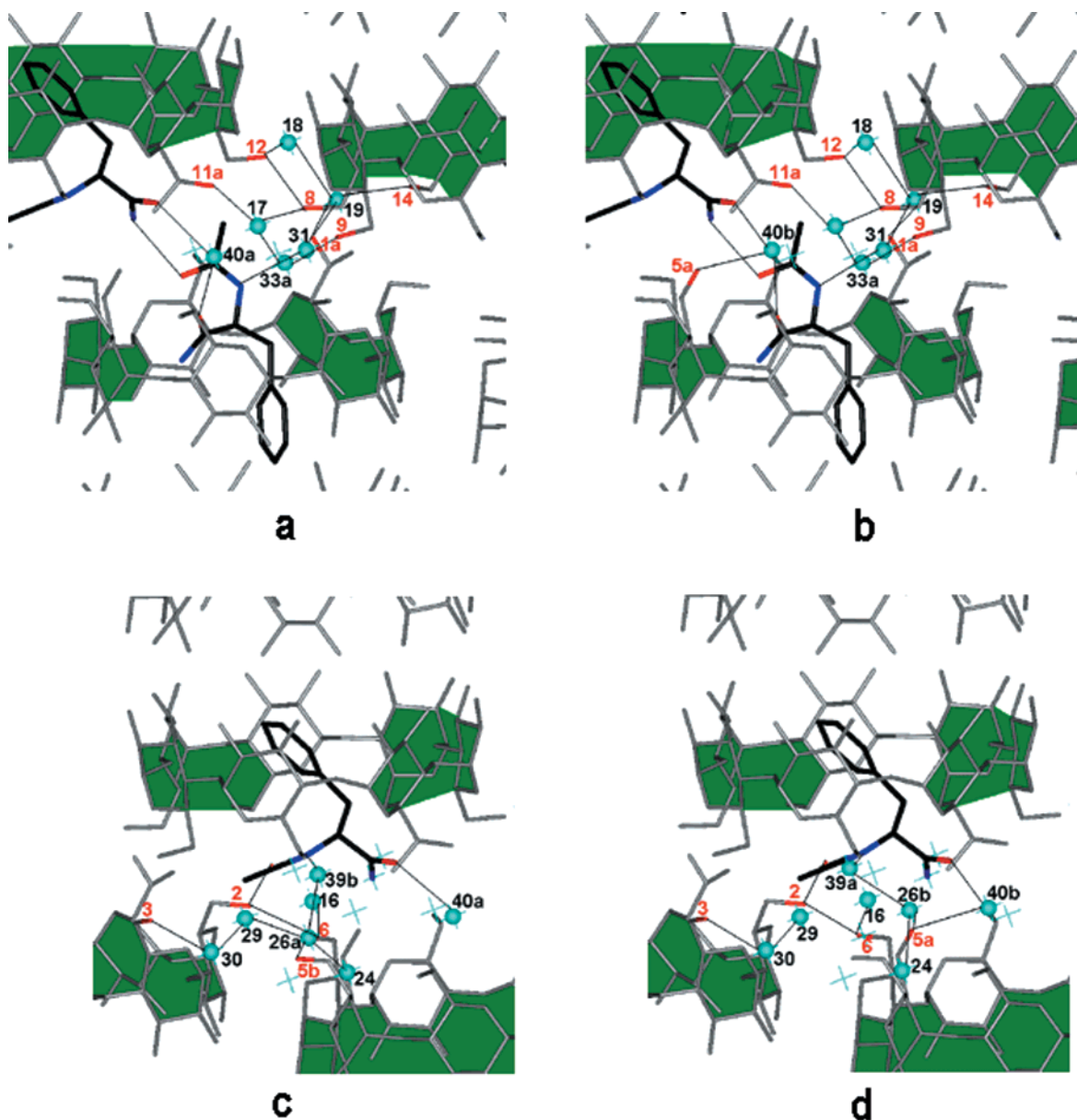


**Figure 6.** Possible hydrogen-bonding interactions for the *N*-acetyl-*L*-phenylalanine amide/ $\beta$ -cyclodextrin complex as observed in the crystal structure. Water atoms are colored cyan and labeled in black; primary hydroxyls are colored and labeled in red. Guest molecules are colored by atom type, with black carbon atoms, blue nitrogen atoms, and red oxygen atoms. Attention is called to water molecules 40a and 40b in (a) and (b); they are disordered but are involved in H-bonds for the disordered guest molecules. Similar attention is called to atoms O6(5a), O6(5b), w26a, w26b, w39a, w39b, w40a and w40b in (c) and (d).

donor to the carbonyl moiety; the latter is not involved in hydrogen bonding.

Intermolecular interactions involving the functional groups at the other end of the pseudopeptide backbones would be expected to differ because of the substituents present. The more hydrophobic ester can serve only as a hydrogen bond acceptor and is a rather weak one at that. The carbonyl oxygen atom of ester molecule **B1** hydrogen bonds directly with hydroxyl oxygen atom O6(5a) of a neighboring  $\beta$ -CD molecule, the same one involved in hydrogen bonding to the acetyl N–H moiety (Figure 5c). The ester moiety of molecule **B2** is not involved in hydrogen bonding. The conformations of the guest molecules in the **A** monomers place the ester groups in the interior of the hydrophobic torus; no evidence for hydrogen bonding is observed.

In the *N*-Ac-*L*-FNH<sub>2</sub> complex, the free amide moiety can serve as a donor, with two sites available, and as an acceptor, with one site available. As illustrated in Figure 6, there is a

hydrogen-bonding interaction between the carbonyl oxygen atoms of the amides in neighboring dimers that is mediated by either of two disordered water molecules (w40a, Figure 6a, or w40b, Figure 6b). The amide NH<sub>2</sub> of the **B** guest acts as a hydrogen bond donor in a direct interaction with the acetyl oxygen of the **A** guest in the dimer below, Figure 6a and b. This direct guest-to-guest hydrogen-bonding interaction is less commonly observed in intermediate packed CD lattices. The backbone of the amide molecule in monomer **B** adopts a different conformation (see Figure 3) than the analogous esters of the *N*-Ac-*L*-FOMe guests to accommodate these hydrogen bond interactions. The decreased apparent thermal motion of the guest molecules in the amide complex is consistent with the increased number of hydrogen-bonding interactions.

A number of additional water molecules in the hydrophilic interdimer binding environment participate in interactions with the host molecules, typically bridging primary hydroxyl groups



of neighboring cyclodextrin molecules. They may be disordered in one crystal structure but not in the other; e.g., water molecule w33 is ordered in the ester complex but disordered in the amide complex, while water w30 is disordered in the ester complex but not in the amide complex.

### Conclusions

As mentioned above, the hydrogen-bonded dimeric cyclodextrin host has previously been characterized as nonconstraining in its interactions with guest molecules. Two features of the crystal structures reported here support that suggestion: (a) the apparently dynamic disorder in the guest molecules in the *N*-Ac-L-FOMe complex and (b) the observed shift in the position of the guest molecule pairs in the *N*-Ac-L-FNH<sub>2</sub> complex in comparison with the former example. It is also noteworthy that there are no hydrogen bond interactions between the guest molecules and the particular host dimer in which they are included. The observation that the hydrophobic interactions between the phenyl rings in a given dimer complex are maintained in the two complexes, even though there is a significant shift in the position of the guest pairs, also supports the idea that the host dimer serves primarily as a nanoscale container for the guest molecules. As such, relatively low energy interactions between guest molecules (such as the C–H– $\pi$  interactions mentioned above) are observed. There is also sufficient room in the extended toroidal void of the hydrogen-bonded host dimer for guest molecules to adopt different conformations. In particular, significantly different backbone conformations are observed in the **A** and **B** monomers for each complex.

The hydrated interface between sheets of essentially close-packed dimer molecules provides an unusual opportunity to examine varied intermolecular hydrogen-bonding interactions. The structures are complex enough to allow variation in hydrogen-bonding schemes adopted by guest molecules whether they have the same or different functional groups, either by introducing crystallographic disorder or as a result of the

crystallographic independence of two chemically identical guest molecules.

Further studies will be necessary to realize the full potential of this model system to contribute to an improved understanding of molecular recognition. Several features in the interactions of the guest molecules with water molecules and with neighboring cyclodextrin molecules have been revealed by this study. This initial study provides grounds for optimism that a meaningful database consisting of a number of crystal structures for energetically similar nonbonding interaction schemes can be assembled. The database should consist of a variety of complexes in which relatively small molecules and waters of hydration interact with a prearranged set of hydrogen bond donors and acceptors in relatively nonconstraining binding environments. Developing an appreciation for the range of the different possibilities will further our understanding of molecular recognition in substrate–macromolecular interactions and in the mechanisms of protein folding as well. Compiling the observed trends in hydrogen-bonding and hydrophilic interactions into a structural database will provide valuable information on the selection of molecular conformations and interactions in nonconstraining binding environments for theoretical computations.

**Acknowledgment.** This work was supported in part by the NSF (CHE-9812146). We thank Tom J. Brett for valuable comments on the refinement and analysis of this system, as well as for assistance with instrumentation.

**Supporting Information Available:** CIF data, ORTEP plots illustrating refined atomic displacement parameters, projections of the five distinct cyclodextrin dimer complex packing types, and a more detailed packing diagram for the Im type. This material is available free of charge via the Internet at <http://pubs.acs.org> JA003717V. See any current masthead page for ordering information and Web access instructions.

JA003717V